Ethylene Homo- and Copolymerization Activity of a Series of [ONNO]-Type Amine Bis(phenolate) Based Vanadium(II–V) Catalysts

Christian Lorber,*[a] Fabien Wolff,[a] Robert Choukroun,[a] and Laure Vendier[a]

Keywords: Vanadium / Amine (bis)phenolates / Polymerization / Copolymer / Crystal structure / Olefins

The synthesis and structural characterization of new paramagnetic amine bis(phenolate) [ONNO]-vanadium(III) and -vanadium(II) complexes, V^{III}(acac)[ONNO], V^{III}(Cl)(THF)[ONNO], and V^{II}(TMEDA)[ONNO], is described. These compounds complete the family of [ONNO]-vanadium(IV/V) complexes previously reported. The members of the [ONNO]-vanadium family at various oxidation states that range from vanadium(II) to vanadium(V), in association with $EtAlCl_2$ cocatalyst, were studied in the polymerization of ethylene and in the copolymerizations of ethylene-1-hexene and ethylene-norbornene. Poly(ethylene-*co*-1-hexene) and poly(-ethylene-*co*-norbornene) were produced with co-monomer content of up to 11 mol-% and 29 mol-% for 1-hexene and norbornene, respectively.

Introduction

In the past decade, a tremendous amount of effort has been devoted to the design of new “non-metallocene” group 4 transition metal complexes because of their importance as α-olefin polymerization catalysts.[1] Particularly, chelating diamide,[1a,2–4] dialkoxide,[1a,5–6] or phenoxyimine[7,8] ligands have been extensively studied as rigid supporting environments for titanium and zirconium complexes, which has resulted in the emergence of a great deal of novel and useful chemistry, including the discovery of highly active olefin polymerization precatalysts. Among these new ligands, chelating, dianionic [ONNO]-type amine bis(phenolate) ligands associated with group 4 metal complexes[5] have proven to be highly active 1-hexene polymerization catalysts, and in some cases, even isospecific living polymerization was possible.[5a] Recently yttrium-[ONNO] complexes have been reported for their catalytic activity in the ring-opening polymerization of ε-caprolactone.[9]

Vanadium-based catalysts in homogeneous Ziegler–Natta polymerization have been known for about half a century.[10] Although generally less active, their use presents a number of interesting advantages over group 4 metal catalysts:[11] (i) the synthesis of high molecular weight polymers with narrow polydispersity, (ii) the preparation of ethylene/α-olefin copolymers with high α-olefin incorporation, and (iii) the preparation of syndiotactic polypropylene. The major reason for the low activity of these systems is their deactivation during the polymerization process, probably due to reduction of the catalytically active vanadium species to low-valent, less active or inactive species. Nevertheless, $V(acac)_3$ is currently employed in the synthesis of EP (ethylene–propylene) and EPDM (ethylene–propylene–diene monomer) elastomers.

As part of an ongoing study of vanadium chemistry with various supporting ligands,[12] and in particular of vanadium complexes for olefin polymerization, we have recently used ancillary diamido ligands with sterically demanding protecting groups[13] or imido ligands[14] on vanadium(IV) complexes as a way to overcome the problem of catalyst deactivation by stabilization of the formal oxidation state of the vanadium center. Following this approach, we recently described the synthesis of a series of oxo-vanadium(V)[15] and vanadium(IV)[16] complexes with the ancillary amine bis(phenolate) [ONNO]-type ligand (Figure 1) that are of the type V^V(=O)(X)[ONNO] {X = O*i*Pr (**1**), N_3 (**2**), Cl (**3**) and V^{IV}(Y)[ONNO] (Y = O*i*Pr (**4**), Cl (**5**)}, and we demonstrated interesting features in the solution and the solid-state structure of these unprecedented complexes. To complete our study on this new family of complexes, we wish to report here on the synthesis, and structural characterization, of new vanadium(III) and vanadium(II) complexes supported by [ONNO]-type bis(phenoxy)amine ligand, and to compare their ethylene homo- and copolymerization activity with other members of the vanadium(II–V) complex family.

Results and Discussion

In previous articles we have described the synthesis of [ONNO]-type amine bis(phenolate) complexes of oxo-vanadium(V) [**1**–**3**] and vanadium(IV) [**4**–**5**].[15,16] Although vanadium complexes with oxidation numbers from +3 to +5 are known to catalyze ethylene polymerization, the active spe-

---

[a] Laboratoire de Chimie de Coordination du CNRS, UPR 8241,
205 route de Narbonne, 31077 Toulouse Cedex 04, France
Fax: +33-5-61-55-30-03
E-mail: lorber@lcc-toulouse.fr

DOI: 10.1002/ejic.200500149

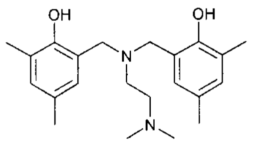

$[ONNO]H_2$

$V^{V}(=O)(OiPr)[ONNO]$	1
$V^{V}(=O)(N_3)[ONNO]$	2
$V^{V}(=O)(Cl)[ONNO]$	3
$V^{IV}(OiPr)_2[ONNO]$	4
$V^{IV}(Cl)_2[ONNO]$	5
$V^{III}(acac)[ONNO]$	6
$V^{III}(Cl)(THF)[ONNO]$	7
$V^{II}(TMEDA)[ONNO]$	8

Figure 1. Structure of [ONNO]-type bis(phenoxy)amine ligand and designation of Vanadium-[ONNO] complexes used in this study.

cies is probably a vanadium(III) complex. Vanadium(II) species are generally considered inactive. To verify this point, we decided to prepare vanadium(III) and vanadium(II) compounds containing the [ONNO] ligand and to test the whole family of [ONNO]-vanadium complexes as olefin polymerization catalysts.

Synthesis of the Vanadium(III) and Vanadium(II) Complexes

Reacting $V(acac)_3$ with 1 equiv. of $[ONNO]H_2$ in toluene at 80 °C for 14 h afforded, after workup, the desired vanadium(III) complex V(acac)[ONNO] (**6**) as an orange solid with 87% yield (Scheme 1). Accordingly, **6** is a d^2-paramagnetic, NMR-silent compound with an effective magnetic moment μ_{eff} of 2.91 μ_B at 20 °C.

$$V(acac)_3 + [ONNO]H_2 \xrightarrow[-\,2\ acacH]{toluene,\ 80\,°C} \underset{\mathbf{6}}{V(acac)[ONNO]}$$

Scheme 1. Synthesis of trivalent complex V(acac)[ONNO].

When 1 equiv. of $K_2[ONNO]$ was slowly added to a THF solution of $VCl_3(THF)_3$ at ambient temperature there was an immediate reaction (Scheme 2). After careful workup and recrystallization in THF/toluene–pentane, yellow crystals of V(Cl)(THF)[ONNO] (**7**) were obtained (yield 31%). As for **6**, complex **7** is NMR-silent, and room temperature magnetic susceptibility measurements gave a μ_{eff} of 2.87 μ_B.

$$VCl_3(THF)_3 + K_2[ONNO] \xrightarrow[-\,2\ KCl]{THF,\ r.t.} \underset{\mathbf{7}}{V(Cl)(THF)[ONNO]}$$

Scheme 2. Synthesis of trivalent complex V(Cl)(THF)[ONNO].

An entry to the [ONNO]-vanadium(II) chemistry was successfully achieved by reacting the vanadium(II) precursor $VCl_2(tmeda)_2$ [tmeda *N,N,N′,N′*-tetramethylethylenediamine] with 1 equiv. of $K_2[ONNO]$ at room temperature whilst stirring in THF for 2 h to give red crystals of complex V(tmeda)[ONNO] (**8**) (Scheme 3). Complex **8** is a high-spin d^3-paramagnetic, NMR-silent compound with a μ_{eff} of 3.90 μ_B at 20 °C.

$$VCl_2(tmeda)_2 + K_2[ONNO] \xrightarrow[\substack{-\,2\ KCl \\ -\,tmeda}]{THF,\ r.t.} \underset{\mathbf{8}}{V(tmeda)[ONNO]}$$

Scheme 3. Synthesis of divalent complex V(tmeda)[ONNO].

X-ray Structure Determination

During the course of our investigation, crystals of $[ONNO]H_2$ were obtained from a cold dichloromethane/pentane solution (–20 °C), and we report its molecular structure with an ORTEP diagram shown in Figure 2.[17] The main features of the solid-state structure is the tripodal configuration that adopts the ligand framework; this arrangement seems to arise from three intramolecular hydrogen-bond interactions between O1–HO1···N1 (2.05 Å, 146.0°), O1–HO1···O2 (2.54 Å, 130.4°), and O2–HO2···N2 (2.03 Å, 151.6°).

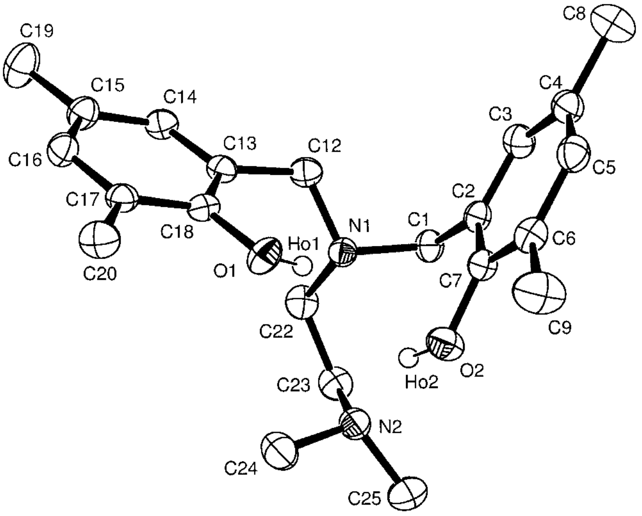

Figure 2. Ortep drawing of the molecular structure of $[ONNO]H_2$ showing 50% probability ellipsoids. Hydrogen atoms are omitted for clarity. Selected parameters (bonds, Å; angles, °): N1–C12 1.467(3), N1–C1 1.482(3), N1–C22 1.473(3), C18–O1 1.371(2), C7–O2 1.367(2), N2–C23 1.462(3), N2–C24 1.467(3), N2–C25 1.465(3), O1–H···N1 2.05, O1–H1···O2 2.54, O2–H2···N2 2.03, O1–H–N1 146.0, O1–H1–O2 130.4, O2–H2–N2 151.6.

Crystals of all three complexes (**6**–**8**) were obtained: red-orange crystals of **6** were obtained by careful layering a toluene solution of **6** with pentane, yellow crystals of **7** by low-temperature crystallization in THF/toluene–pentane solution, and red crystals of **8** by layering a toluene solution of **8** with pentane. The thermal ellipsoid plots are depicted in Figure 3, Figure 4, and Figure 5, with a comparison of selected bond lengths and angles in Table 1. Complex **8** presents two independent molecules in the cell with very similar structural parameters; therefore only one of these molecules will be described here. The solid-state structures confirm our first formulations: complexes **6**–**8** are mononuclear complexes, containing an octahedrally coordinated vanadium(III) center surrounded by a tetradentate [ONNO] ligand and one acac ligand (**6**), a chlorine atom and a THF solvate molecule (**7**), and tmeda ligand (**8**). With regard to the [ONNO] ligand, in all complexes, the two phenolate rings have a *trans* configuration, and both amino-nitrogen donor atoms are coordinated to the metal center; these features are ones that they share with their group 4- and other vanadium-[ONNO] analogues.[5b,5d–f,15,16] Bonding distances between the metal center and the O and N donors of [ONNO] are in the range typically observed for such complexes: (i) V–O(phenoxide) distances are ca. 1.9–2.0 Å, which is slightly longer than those of higher oxidation state [ONNO]-vanadium(V/IV) analogues by about 0.1 Å,[14,15] (ii) the two vanadium–nitrogen bonds formed between the metal center and the tripodal amino-N atom and the dimethylamino sidearm N atom have distances that range from 2.13 to 2.32 Å. Bonds formed by vanadium and the additional ligands are typical: V–O(acac) approximately 2.00 Å (in **6**), V–Cl1 = 2.377(2) Å (in **7**), V–O(THF) = 2.131(4) Å (in **7**), and V–N(TMEDA) = 2.302(8) and 2.383(8) Å (in **8**).

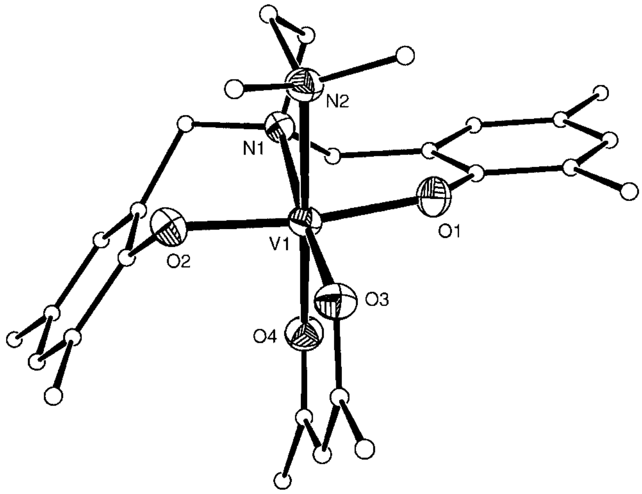

Figure 3. Ortep drawing of the molecular structure of **6** showing 50% probability ellipsoids (except on C atoms for clarity) and partial atom-labeling schemes. Hydrogen atoms are omitted for clarity.

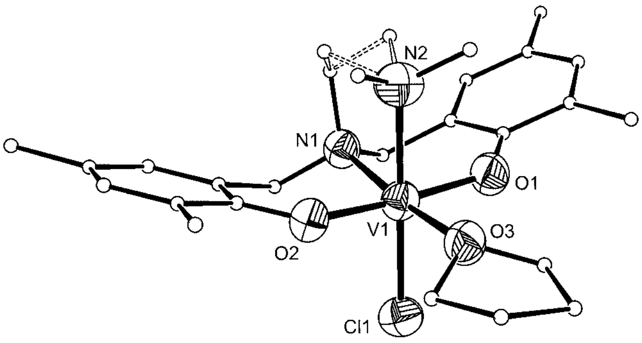

Figure 4. Ortep drawing of the molecular structure of **7** showing 50% probability ellipsoids (except on C atoms for clarity) and partial atom-labeling schemes. Hydrogen atoms are omitted for clarity.

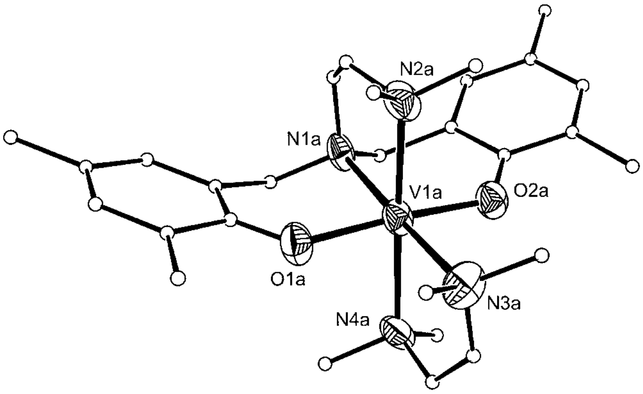

Figure 5. Ortep drawing of the molecular structure of molecule A of **8** showing 50% probability ellipsoids (except on C atoms for clarity) and partial atom-labeling schemes. Hydrogen atoms are omitted for clarity.

The crystals of **7** contain the isomer with the chlorine atom *trans* to the dimethylaminoethyl sidearm and the THF ligand *trans* to the tripodal nitrogen atom of [ONNO]. However, because of the paramagnetism of the complex and the impossibility of recording its NMR spectrum we cannot exclude the presence of the other isomer (with the Cl atom *trans* to the tripodal N atom) in solution.

Interestingly, the configuration of the [ONNO] fragment in the crystal structure of **6** is very different from that of **7** and **8**. The configuration of the [ONNO] ligand in **7** and **8**

Table 1. Selected structural parameters for complexes **6**–**8** (distances are given in Å and angles in °).[a]

	V(acac)[ONNO] (**6**)	V(Cl)(THF)[ONNO] (**7**)	V(tmeda)[ONNO] (**8**)[b]
V–O1	1.9179(12)	1.895(4)	2.060(7)
V–O2	1.9317(12)	1.906(4)	2.065(7)
V–N1	2.2020(14)	2.126(4)	2.215(8)
V–N2	2.2147(14)	2.233(5)	2.322(8)
V–X1	1.9761(13) (*O3*)	2.377(2) (*Cl1*)	2.302(8) (*N3*)
V–X2	1.9979(12) (*O4*)	2.131(4) (*O3*)	2.383(8) (*N4*)
O1–V–O2	170.15(5)	173.90(18)	174.1(3)
N1–V–N2	82.62(5)	82.29(17)	79.3(3)
X1–V–X2	90.34(5)	91.73(12)	80.5(3)
V–O1–$C_{phenolate}$	135.4(1)	132.7(4)	130.3(7)
V–O2–$C_{phenolate}$	116.2(1)	132.9(3)	130.1(6)
δ[c]	+132	–142	–150

[a] X1 = X2 = O_{acac} (**6**) or N_{tmeda} (**8**); X1 = Cl, X2 = O_{THF} (**7**). [b] For independent molecule A. [c] Angle defined by the two planes containing the two phenolate aromatic rings; the + sign refers to a folding away from the NMe_2 sidearm, whereas the – sign refers to a folding towards the NMe_2 sidearm.

is symmetry related [the two aromatic rings of the bis(phenolate) framework (without the sidearm)]; the phenolate groups of the [ONNO] framework fold in towards the pendant (dimethylamino)ethyl sidearm, and the angle between the two planes of the aromatic rings are approximately –142° (**7**) and –151° (**8**) [the minus sign refers to a folding towards the NMe_2 sidearm; in contrast, the folding away from the NMe_2 sidearm has a positive sign]. In contrast, the phenolate groups of the [ONNO] ligand of **6** fold back away from the pendant (dimethylamino)ethyl sidearm; the angle δ between the two planes of the aromatic rings is now about +116° with a molecular structure that has two non-symmetry-related phenolate rings. Such a helicoidal distortion of the tripodal amino nitrogen donor atom induces a lower symmetry in the ligand framework of **6**, as already observed in the solid-state structure of two other [ONNO]-vanadium complexes,[15,16] and seems to arise from the presence of an O-ligated anionic ligand (alkoxo, oxo, acac) in a *trans* position to the (dimethylamino)ethyl sidearm nitrogen donor atom. Figure 6 presents a summary of the geometry of all the [ONNO]-vanadium compounds that we have prepared.

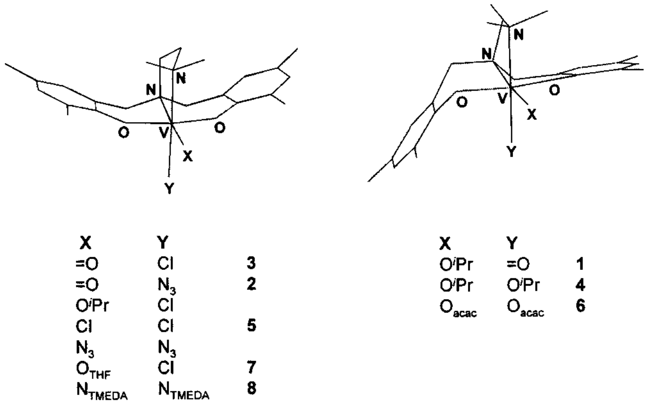

X	Y	
=O	Cl	3
=O	N_3	2
O^iPr	Cl	
Cl	Cl	5
N_3	N_3	
O_{THF}	Cl	7
N_{TMEDA}	N_{TMEDA}	8

X	Y	
O^iPr	=O	1
O^iPr	O^iPr	4
O_{acac}	O_{acac}	6

Figure 6. Symmetrical and non-symmetrical geometry in [ONNO]-Vanadium(II–IV) complexes.

Homopolymerization Studies

Together with the [ONNO]-vanadium complexes that present oxidation states of +5 and +4 reported by us in previous articles,[15,16] we are now introducing a family of vanadium complexes that are supported by the same ancillary ligand and that stabilize four oxidation states of the metal center (from +2 to +5), which allows us the opportunity to evaluate their activity toward the homopolymerization of ethylene, propene, and 1-hexene.

Ethylene Polymerization

Preliminary studies conducted on **6** with MAO cocatalyst (500 equiv.) under 1 bar of ethylene failed to produce polyethylene. We had already observed such behavior with other vanadium catalysts that do not possess V–Cl bonds.[14] Moreover, it is well known that vanadium catalysts give higher polymerization activities or polymers with lower polydispersity indices upon activation with simple chloroalkylaluminum reagents (such as $EtAlCl_2$ or Et_2AlCl) rather than MAO.[11b,11c,14,18,19] As a result, all of our further studies were conducted with $EtAlCl_2$ as cocatalyst.

The catalyst activity of the vanadium(II–V) complexes **1**–**8** of the [ONNO] ligand for the polymerization of ethylene has been evaluated under the same set of conditions of 10 equiv. of $EtAlCl_2$ under 1 atm of ethylene at 20 °C in toluene (except for catalysts **2** and **3** that are not soluble in toluene, and these reactions were thus conducted in dichloromethane). The results are summarized in Table 2 and are classified by the oxidation states of the catalysts; a comparison with standard V-based catalysts VCl_4, VCl_4·DME, and $V(acac)_3$ tested in our hands under the same experimental conditions is also presented.

Under these conditions, [ONNO]-vanadium(V) complexes **2** and **3** exhibit modest activities ranging from 17 to 22 $kg_{PE}\,mol^{-1}{}_{[V]}\,h^{-1}$, a number comparable to other vanadium systems described in the literature.[1a,11,14,18] This modest activity may be attributable to the use of dichloromethane as solvent; catalyst **1** gives a much higher produc-

Table 2. Ethylene polymerization promoted by various vanadium catalysts [conditions: catalyst (about 10 mg, ca. 0.01 mmol) in 10 mL of solvent; $EtAlCl_2$ cocatalyst (10 equiv.); ethylene (1 bar); time of polymerization 15 min run, except when the solution solidifies to give a polymer gel, the asterix (*) denotes such a reaction].

Catalyst	Solvent	Time [min]	Yield [mg]	Activity[a]	T_m [°C][b]	M_w [g/mol × 10^{-3}][c]	M_n [g/mol × 10^{-3}][c]	M_w/M_n[c]
$V^VO(O^iPr)$[ONNO] (**1**)	toluene	5*	227	272	134.0	118	44	2.65
$V^VO(N_3)$[ONNO] (**2**)	CH_2Cl_2	15	55	22	138.7	146	32	4.60
$V^VO(Cl)$[ONNO] (**3**)	CH_2Cl_2	15	42	17	136.4	716	190	3.76
$V^{IV}(O^iPr)_2$[ONNO] (**4**)	toluene	3*	237	474	138.7	677	338	2.00
$V^{IV}(Cl)_2$[ONNO] (**5**)	toluene	15	156	62	139.0	889	438	2.03
VCl_4	toluene	10*	373	22	135.1	152	19	8.13
VCl_4·DME	toluene	4*	250	200	137.5	152	48	3.19
$V^{III}(acac)$[ONNO] (**6**)	toluene	3*	218	436	133.4	673	202	3.33
$V^{III}(acac)$[ONNO] (**6**)	pentane	5*	268	322	128.5	1003	381	2.63
$V^{III}(Cl)(THF)$[ONNO] (**7**)	toluene	15	129	52	135.2	458	204	2.24
$V(acac)_3$	toluene	10*	141	85	135.8	176	72	2.43
$V^{II}(tmeda)$[ONNO] (**8**)	toluene	15	4	1	–	2259	745	3.03

[a] In $kg_{PE}\,mol^{-1}\,h^{-1}\,atm^{-1}$. [b] Determined by DSC. [c] Determined by SEC in 1,2,4-trichlorobenzene at 140 °C versus polystyrene standards.

tivity of 272 $\mathrm{kg_{PE}\,mol^{-1}{}_{[V]}\,h^{-1}}$. Polymer properties are typical of high molecular weight (M_w = 1.18–7.16×10^5 $\mathrm{g\,mol^{-1}}$), high density polyethylenes [HDPE] (T_m = 134–139 °C), and a reasonably narrow, unimodal polydispersity indice, M_w/M_n = 2.65, is observed with **1**.

Under the above conditions, the activities of the vanadium(IV)-[ONNO] catalysts **4** and **5** are much higher; 474 $\mathrm{kg_{PE}\,mol^{-1}{}_{[V]}\,h^{-1}}$ (**4**) and 62 $\mathrm{kg_{PE}\,mol^{-1}{}_{[V]}\,h^{-1}}$ (**5**). Meanwhile, polydispersity indices are very low (2.00 and 2.03, respectively), which suggests that the active species is well defined, and the [ONNO] ligand remains coordinated to the metal during the catalytic process. Melting temperatures are again very high (ca. 139 °C) corresponding to HDPE.

Vanadium(III)-[ONNO] catalyst **6** is a particularly efficient catalyst; as with **4**, a rapid initial polymerization occurs, which results in the solidification of the solution with formation of a gel of PE in less than 2 min (activity = 436 $\mathrm{kg_{PE}\,mol^{-1}{}_{[V]}\,h^{-1}}$). This problem could be partly resolved by conducting the reaction in pentane. We then observe a slightly lower productivity, but a gain in the polydispersity (3.33 in toluene versus 2.63 in pentane), and a high molecular weight polymer (M_w = 1.00×10^6 $\mathrm{g\,mol^{-1}}$). Interestingly, ethylene polymerization with the other vanadium(III) catalyst **7** is a little bit slower than with **6**, although the low polydispersity (2.24) suggests again a well-defined active species.

Finally, vanadium(II) complex **8** gives poor yields of PE. As expected, this confirms that this reduced oxidation state of the vanadium center gives only inactive or less active polymerization catalysts. Nevertheless, one cannot exclude that the absence of activity is due to the presence of the chelating TMEDA ligand at the metal center, and additional polymerization experiments with vanadium(III–V) catalysts in the presence of TMEDA will be necessary to address this point.

Although clear trends are not easily apparent (except for the V^{II} state that is inactive), the following conclusion can be drawn: (i) catalysts **2**, **3**, **5**, and **7** with V–Cl or V–N_3 bonds give lower activities relative to catalysts **1**, **4**, and **6** that have alkoxide or acac ligands, (ii) the activities and quality of the polyethylenes obtained with catalysts **1**, **4**, and **6** (with oxidation states +5 to +3) are very similar. This could suggest that these different systems involve a similar catalytically active species that is most probably a [ONNO]-vanadium(III) complex (in the case of **1** and **4**, resulting from the reduction of the V^V or V^{IV} center by the aluminum cocatalyst). Clearly, further studies will be needed to clarify these points.

Propene and 1-Hexene Homopolymerization

Unfortunately, none of the [ONNO]-vanadium complexes could catalyze propene polymerization at 20 °C, even under 4 bar propene, using $EtAlCl_2$ as cocatalyst (V/Al = 1:10). This is surprising as the $V(acac)_3/EtAlCl_2$ system is known to initiate living propene polymerization,[20] but this may result from the strong steric hindrance of the tetradentate dianionic [ONNO] ligand.

Less surprisingly, we were unable to polymerize 1-hexene with our catalysts, even at high temperatures (70 and 135 °C). To the best of our knowledge, V-based catalysts reported for such a reaction are very rare.[21]

Ethylene Copolymerization Studies

The copolymerization of ethylene with α-olefins is a common means of generating polyethylenes with controlled crystallinity and density. These polymers are known as linear low-density polyethylenes (LLDPE). The introduction of short-chain branches originating from the co-monomer decreases the crystallinity and melting temperature of the copolymer as the co-units interfere with crystallization and reduce the size of crystallites. Preliminary studies of the copolymerization of ethylene with 1-hexene and norbonene with our new vanadium compounds are described below.

The copolymerization of ethylene with 1-hexene was conducted at ambient temperature in toluene with complexes **1** and **4**–**7** in the presence of $EtAlCl_2$ cocatalyst (V/Al = 1:10), under 2 bar ethylene with a ratio of 1:800 for catalyst/1-hexene, and was compared to that of $V(acac)_3$ (see Table 3).

Although **7** did not produce any polymer, a white polymeric material was obtained with the other catalysts **1** and **4**–**6**. The ^{13}C NMR spectra (370 K) of the resulting polymers reveals that these catalysts produced poly(ethylene-*co*-hexene)s (EH) typical of EH block copolymers, and the polyethylene sequences are separated by isolated hexene units (no HH dyads are observed; Figure 7 shows a

Table 3. Results of ethylene–1-hexene copolymerization [conditions: catalyst (0.01 mmol) in 10 mL of toluene; $EtAlCl_2$ cocatalyst (10 equiv.); ethylene (2 bar); 1-hexene (8 mmol); time of polymerization 30 min run].

Catalyst	Yield [mg]	Activity[a]	T_m [°C][b]	1-Hexene content [mol%][c]	M_w [g/mol × 10^{-3}][d]	M_n [g/mol × 10^{-3}][d]	M_w/M_n[d]
1	354	78	73.5, 83.6, 92.7, 96.8, 104.2, 120.7	4.0	32	7.6	4.26[e]
4	60	12	62.5, 72.1, 81.1, 91.6, 102.2, 111.2	3.5	73	21	3.53
5	192	38	63.0, 72.6, 82.8, 92.5, 96.1, 105.6, 117.9	4.2	–	–	–
6	600	120	63.5, 73.0, 83.0, 93.1, 107.3	7.4	71	41	1.70
6[f]	702	140	63.3, 72.9, 82.4, 92.6, 103.0, 109.6	3.6	149	72	2.07
6[g]	303	61	62.3, 72.2, 81.9, 91.3, 102.5, 107.1	10.6	33	17	1.90
$V(acac)_3$	838	167	63.6, 73.2, 83.2, 92.9, 103.1, 119.8	7.5	2882	13	225.52

[a] In $\mathrm{kg_{PE}\,mol^{-1}\,h^{-1}}$. [b] Determined by DSC. [c] Determined by ^{13}C NMR spectroscopy (370 K). [d] Determined by SEC in 1,2,4-trichlorobenzene at 140 °C versus polystyrene standards. [e] Bimodal distribution. [f] Ethylene (4 bar). [g] Ethylene (1 bar).

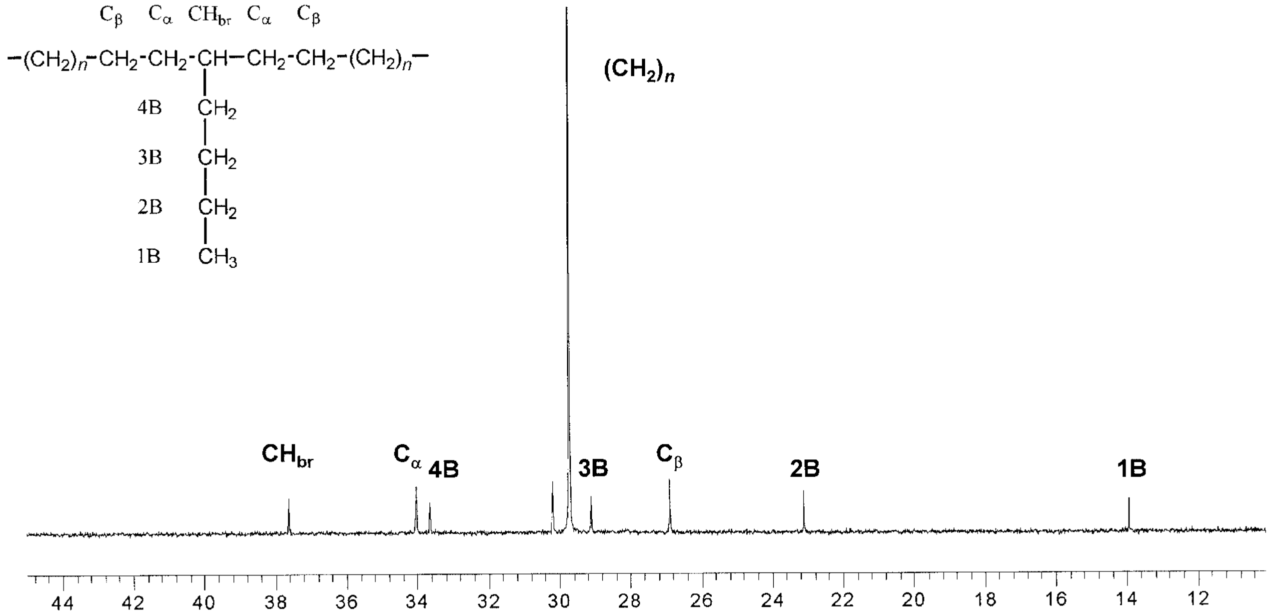

Figure 7. ^{13}C NMR spectrum [370 K, 1,2,4-trichlorobenzene/[D$_2$]tetrachloroethane] of the ethylene–*co*-1-hexene polymer made using **6**/EtAlCl$_2$.

$^{13}C\{^1H\}$ NMR spectrum of an EH copolymer obtained using **6**/EtAlCl$_2$).

The integration of the signals of 1-hexene versus ethylene in the ^{13}C NMR spectra of these EH copolymers allowed us to determine the 1-hexene incorporation ratio into the copolymers.[22] This value was found to be relatively modest, ca. 4 mol%, with catalysts **1**, **4** and **5**, and slightly higher with **6** (7.4 mol%). Increasing the ethylene pressure to 4 bar (with catalyst **6**) resulted in a decrease in catalyst productivity, whereas (logically) the 1-hexene content diminished to 8.8 mol%. Conversely, lowering the ethylene pressure to 1 bar decreased the activity with incorporation of more 1-hexene units (10.6%). These conditions have not been optimized; in particular, we have also noticed an increase in the 1-hexene content and productivity of **6** by working in a pentane solution.

In all cases, the EH copolymers have a low molecular weight M_w of 32×10^3 (with **1**), 73×10^3 (with **4**) and 71×10^3 (with **6**), but with different molecular weight distributions; the EH copolymers produced by **1** and **4** have a broad molecular weight distribution [PDI = 4.26 (bimodal), and 3.53 for **1**, and **4**, respectively], whereas narrow unimodal polydispersity indices are obtained with **6** at various ethylene pressures [PDI = 1.90 (1 bar), 1.70 (2 bar), and 2.07 (4 bars)].

The effect of the incorporation of 1-hexene into the copolymer on the melting behavior of the EH copolymer is illustrated in Figure 8, which shows the DSC endotherms obtained after step-crystallization of the copolymers made using **6**/EtAlCl$_2$. Furthermore, it has been established that 1-hexene does not enter the crystal lattice of PE, therefore, a DSC analysis can give an idea of the heterogeneity in the co-monomer distribution.[23,24] The DSC thermograms of the EH copolymers show five to six melting temperature values ranging from ca. 63 °C to ca. 111 °C. According to these endotherms, and those found in the literature,[23,24] separations based on different populations of crystalline lamellae have occurred, depending on the amount and distribution of 1-hexene units in the molecular chain ("intrachain heterogeneity"). Long polymer segments recrystallize into larger crystals, which melt at higher temperatures, whereas short segments form small crystals, which melt at lower temperatures. Each peak of the DSC curve corresponds to one type of polymer fraction, which could have a different amount and distribution of short-chain branching in the PE chain.

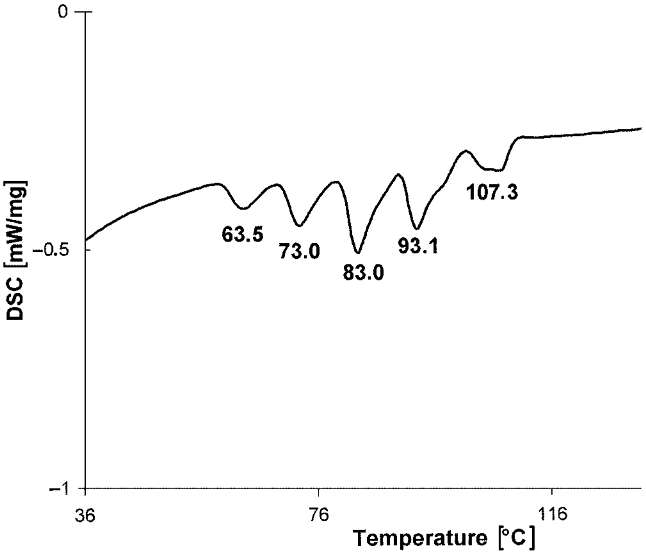

Figure 8. DSC thermogram obtained for an ethylene–*co*-1-hexene polymer made using **6**/EtAlCl$_2$.

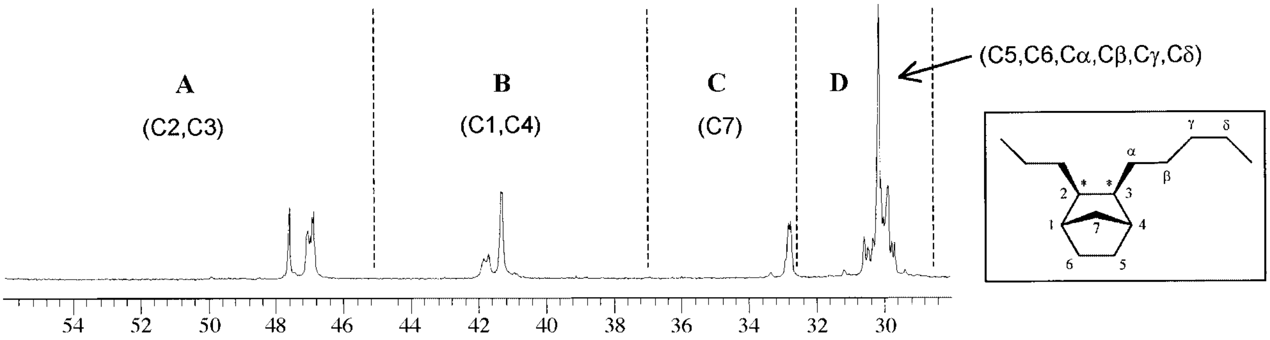

Figure 9. ^{13}C NMR spectrum [370 K, 1,2,4-trichlorobenzene–[D_2]tetrachloroethane] of the ethylene–*co*-norbornene polymer made using **6**/$EtAlCl_2$ (ethylene 1 bar).

As materials, poly(ethylene-*co*-norbornene)s possess rather interesting properties (high glass transitions, good chemical and heat resistance, and excellent transparency) that make them promising, in particular, for their potential applications in optoelectronics. Under the above conditions used to produce the poly(ethylene-*co*-hexene) [room temperature, and 1–4 bar ethylene, in the presence of norbornene], preliminary studies show that **6** associated with $EtAlCl_2$ (V/Al = 1:10) presents an interesting catalytic activity for ethylene–norbornene copolymerization (Table 4): activity = 292 $kg_{copolymer}\,mol^{-1}\,h^{-1}$ at 2 bar ethylene. The resultant polymer was poly(ethylene-*co*-norbornene) with a similar overall ^{13}C NMR spectrum (see Figure 9), high norbornene content (14–29 mol%),[25] and a microstructure that possesses no norbornene repeat units and contains both *meso* and *racemo* alternating ethylene–norbornene sequences as well as isolated norbornene units. More details on the copolymerization behavior of these systems will be described elsewhere.

Table 4. Results of ethylene–norbornene copolymerization [conditions: catalyst (0.01 mmol) in 10 mL of toluene; $EtAlCl_2$ cocatalyst (10 equiv.); ethylene (1–4 bar); 1-hexene (8 mmol); time of polymerization 15 or 30 min run].

Catalyst	*P* [bar]	Time [min]	Yield [mg]	Activity[a]	Norbornene content [mol%][b]
6	1	30	329	66	29
6	2	15	730	292	18
6[c]	4	15	868	347	14

[a] In $kg_{PE}\,mol^{-1}\,h^{-1}$. [b] Norbornene content in mol% determined by ^{13}C NMR spectroscopy (370 K). [c] Toluene (20 mL).

Conclusions

We described the synthesis and molecular structure of three new amine(bisphenolate) complexes of vanadium(II) and (III). We used the whole family of [ONNO]-vanadium complexes, from vanadium(II) to vanadium(V), as ethylene polymerization catalysts in association with the $EtAlCl_2$ cocatalyst. To the best of our knowledge, this is the first comprehensive study of a catalytic polymerization system with a single ancillary ligand set to stabilize such a broad scale of oxidation states of the metal center.

Preliminary studies show that some of these new complexes are efficient catalysts for ethylene-α-olefin copolymerization, producing poly(ethylene-*co*-1-hexene) and poly(ethylene-*co*-norbornene) with high α-olefin content. These promising results still need to be optimized, and future studies are in progress to determine the best catalytic conditions (temperature, ethylene pressure, co-monomer and cocatalyst concentration), as well as the effect of halogenated compounds as activity enhancers.[26] These studies will appear in due course. From our preliminary polymerization results, and because it is easily prepared from commercially available $V(acac)_3$, $V^{III}(acac)[ONNO]$ appears as the most interesting complex for further studies. Our study also confirms the importance of the vanadium(III) as the active species in V-based catalytic systems.

Experimental Section

General Remarks: Starting materials for ligand synthesis were purchased from Aldrich Inc. or Fluka Inc. and used as received. All experiments requiring a dry atmosphere were performed using standard Schlenk line or drybox techniques under argon. Solvents were refluxed and dried over appropriate drying agents under argon, collected by distillation, and stored in the drybox over 4 Å molecular sieves. The ligand $[ONNO]H_2$ was prepared according to a known synthesis.[5e] $K_2[ONNO]$ was prepared by adding excess K into a THF solution of $[ONNO]H_2$, filtering and evaporating to dryness. $V(acac)_3$ was purchased from Fluka. $EtAlCl_2$ (25 mol-% in toluene) was purchased from Aldrich. All vanadium precursors $VCl_3(THF)_3$ and $VCl_2(tmeda)_2$ were prepared as published previously.[27,28] [ONNO]-vanadium(V) and -vanadium(IV) complexes were prepared according to published syntheses.[15,16] NMR spectroscopic data were recorded with a AMX-400 spectrometer, and referenced internally to residual protonated-solvent (^1H) resonances and are reported relative to tetramethylsilane (δ = 0 ppm). Pseudo-quantitative ^{13}C NMR spectra of the copolymers were obtained at 370 K in 1,2,4-trichlorobenzene/[D_2]tetrachloroethane containing approximately 3 mg of $Cr(acac)_3$ to reduce T_1 (inverse-gated, $d1$ = 5 s). Co-monomer incorporation was measured by integration of characteristic signals. Elemental analyses were performed at the Laboratoire de Chimie de Coordination (Toulouse, France). Magnetic susceptibility data were collected on powdered samples of the different compounds with use of a homemade Faraday-type automatic magnetometer with mercury tetra(thiocyanato) cobaltate susceptibility at 20 °C, $16.44\times10^{-6}\,cm^3\,mol^{-1}$). Diamagnetic corrections were applied by using Pascal's constants as described previously.[12b] Size exclusion chromatography (SEC) analyses were carried out at the CNRS-LCPO laboratory (Bordeaux-Pessac, France) and at Polimeri Europa (Milan, Italy) in 1,2,4-trichlorobenzene at 140 °C relative to polystyrene standards. DSC thermograms of the polymers were measured on a DSC 204 Netzsch apparatus using a modified method.[29] The polymer sample was melted in a DSC crucible at 170 °C under nitrogen (10 °C/min). It was then successively annealed under nitrogen at descending temperature stages, starting from the melt by steps of 10 °C to reach 20 °C (with isotherms of 2 h between 110 and 60 °C). The cooled sample was then heated at 5 °C/min from 20 to 200 °C (the melting temperature values T_m and the heat of fusion (ΔH_f) were taken from the second heating curve).

Synthesis of V^{III}(acac)[ONNO] (6): To a solution of $V(acac)_3$ (100 mg, 0.29 mmol) in toluene (2 mL) was added $[ONNO]H_2$ (102 mg, 0.29 mmol) in portions at room temperature. The reaction mixture was heated at 80 °C for 14 h, after which the volatiles were removed under vacuum. The resulting orange solid was washed with pentane (3×5 mL) and dried under vacuum. Yield: 128 mg, 87%. μ_{eff} (20 °C) = 2.91 μ_B. $C_{27}H_{37}N_2O_4V$ (504.54): calcd. C 64.27, H 7.39, N 5.55; found C 64.02, H 7.24, N 5.69.

Synthesis of V^{III}(Cl)(THF)[ONNO] (7): K_2[ONNO] (174 mg) was slowly added in portions to a solution of $VCl_3(THF)_3$ (150 mg, 0.41 mmol) in THF (2 mL). The solution was left at ambient temperature whilst stirring overnight. Volatiles were removed under vacuum. The resulting solid was extracted with toluene, the solution was filtered through Celite and dried in vacuo. The solid was washed with pentane and dried under vacuum. Crystallization from a THF/toluene–pentane solution (room temperature and then at –20 °C) afforded yellow crystals of **7**. Yield: 65 mg, 31%. μ_{eff} (20 °C) = 2.87 μ_B. $C_{26}H_{38}ClN_2O_3V$ (512.99): calcd. C 61.87, H 7.47, N 5.46; found C 62.07, H 7.15, N 5.11.

Synthesis of V^{II}(tmeda)[ONNO] (8): K_2[ONNO] (366 mg) was slowly added in portions to a solution of $VCl_2(TMEDA)_2$ (300 mg, 0.84 mmol) in THF (4 mL), whilst stirring. After 2 h at room temperature, the volatiles were removed under vacuum. The resulting solid was extracted with toluene (5 mL), the solution was filtered through Celite and slowly layered with pentane (7 mL). Red crystals of **8** were obtained and dried under vacuum. Yield: 200 mg, 46%. μ_{eff} (20 °C) = 3.90 μ_B. $C_{28}H_{46}N_4O_2V$ (521.63): calcd. C 63.47, H 8.89, N 10.74; found: C 63.40, H 8.70, N 10.66.

Typical Ethylene Polymerization Catalyses: A 10 mL toluene solution of catalyst (5 mg) was flushed under 1 bar ethylene. The $AlEtCl_2$ (10 equiv. of a 1 M solution in toluene) cocatalyst dissolved in toluene (1.5 mL) was added to initiate the polymerization, and the ethylene pressure was maintained constant during the polymerization. The polymerization was stopped by adding methanol (5 mL), and the polyethylenes were filtered, washed with methanol, water and acetone, and dried for 48 h at 80 °C.

Typical Ethylene-α-olefin Copolymerization Catalyses: A 10 mL toluene solution of catalyst (5 mg) and 1-hexene (680 mg) [or norbornene (760 mg)] was flushed under 2 bar ethylene. The $AlEtCl_2$ (10 equiv. of a 1 M solution in toluene) cocatalyst dissolved in toluene (1.5 mL) was added to initiate the polymerization, and the ethylene pressure was maintained constant during the polymerization. The polymerization was stopped by adding methanol (5 mL), and the polyethylenes were filtered, washed with methanol, water and acetone, and dried for 48 h at 80 °C.

Crystal Structure Determination of $[ONNO]H_2$ and 6–8: (Table 5) For the four compounds, data were collected at low temperature (T = 180 K) with a Stoe Imaging Plate Diffraction System (IPDS), equipped with an Oxford Cryosystems Cryostream Cooler Device and using a graphite-monochromated Mo-K_α radiation (λ = 0.71073 Å). Final unit cell parameters were obtained by means of a least-squares refinement of a set of 8000 well-measured reflections, and the crystal decay was monitored during data collection by measuring 200 reflections by image; no significant fluctuation of intensities was observed. Structures were solved by means of

Table 5. Crystal data and structure refinement parameters for $[ONNO]H_2$ and **6**–**8**.

	$[ONNO]H_2$	**6**	**7**	**8**
Chemical formula	$C_{22}H_{32}N_2O_2$	$C_{27}H_{37}N_2O_4V$	$C_{26}H_{38}ClN_2O_3V$	$C_{56}H_{92}N_8O_4V_2$
Formula weight	356.50	504.53	512.97	1043.26
Crystal system	orthorhombic	monoclinic	monoclinic	monoclinic
Space group	$P2_12_12_1$	$P2_1$	$P2_1/c$	$P2_1/c$
a [Å]	8.457(5)	7.780(2)	11.660(5)	13.135(5)
b [Å]	14.127(5)	20.859(4)	20.125(5)	13.516(5)
c [Å]	17.023(5)	8.596(2)	11.737(5)	32.246(5)
α [°]	90	90	90	90
β [°]	90	112.780(3)	102.444(5)	91.517(1)
γ [°]	90	90	90	90
V [Å]^3	2033.7(15)	1286.2(5)	2689.5(18)	5724(3)
Z	4	2	4	8
$D_{calcd.}$ [g cm^{-3}]	1.164	1.303	1.267	1.201
μ (Mo-K_α) [mm^{-1}]	0.074	0.420	0.496	0.377
F(000)	776	536	1088	2248
2θ range [°]	5.6–52.6	5.1–51.8	4.0–46.5	4.00–46.6
Measured reflections	15550	11887	15570	30871
Unique reflections/R_{int}	2371/0.0715	4747/0.0209	3849/0.0967	7893/0.1393
Parameters/restraints	243/0	315/1	313/3	648/21
Final R indices [$I>\sigma 2(I)$]	R_1 = 0.0409, wR_2 = 0.0929	R_1 = 0.0238, wR_2 = 0.0621	R_1 = 0.0576, wR_2 = 0.1328	R_1 = 0.1391, wR_2 = 0.3381
Final R indices all data	R_1 = 0.0524, wR_2 = 0.0981	R_1 = 0.0246, wR_2 = 0.0626	R_1 = 0.1135, wR_2 = 0.1581	R_1 = 0.1587, wR_2 = 0.3518
Flack parameter	–	–0.003(11)	–	
Goodness of fit	1.025	1.025	0.920	1.141
$\Delta\rho_{max} - \Delta\rho_{min}$ [e Å^3]	0.150 and –0.170	0.177 and –0.203	0.468 and –0.327	0.750 and –0.919

direct methods with the programs SIR92/97,[30] and subsequent difference Fourier maps and models were refined by least-squares procedures on F^2 by using SHELXL-97[31] integrated in the package WINGX version 1.64,[32] and empirical absorption corrections were applied to the data.[33] All hydrogen atoms were located on differences Fourier maps and introduced in the refinement as fixed contributors using a riding model with an isotropic thermal parameter fixed at 20% higher than those of the C sp^2 atoms and 50% for the C sp^3 atoms to which they were connected. Methyl groups they were refined with the torsion angle as a free variable. For the three compounds, all non-hydrogen atoms were anisotropically refined, and in the last cycles of refinement, weighting schemes were used, where weights are calculated from the following formula: $w = 1/[\sigma^2(F_o^2) + (aP)^2 + bP]$, where $P = (F_o^2 + 2F_c^2)/3$. In the case of compound **6**, with a polar space group ($P2_1$), SHELXL automatically generates floating origin restraints to fix the X-ray 'centre of gravity' of the structure in the polar axis direction (in the case of $P2_1$, with unique axis *b*, the polar axis is *Y*). Complex **8** presents two independent molecules in the cell with very similar structural parameters. The crystal structure of **8** refined to a high *R* factor because of poor quality, probably as a result of multilayer-type crystals (considering the reciprocal), which could not be treated as twin crystals. The resulting R_{int} was very high (13.93%), which explains the poor final *R* value. The final residues (with low values $+0.90 < Q < -0.95$) are all located close to the metal centers.

CCDC-263761, –263762, –263763 and CCDC-263764 contain the supplementary crystallographic data for this paper. These data can be obtained free of charge from The Cambridge Crystallographic Data Centre via www.ccdc.cam.ac.uk/data_request/cif.

Acknowledgments

This research was supported by the Centre National de la Recherche Scientifique (CNRS). Prof. H. Cramail (Bordeaux, France) and Dr. G. Conti (Polimeri Europa, Milan, Italy) are thanked for the SEC.

---

[1] For recent reviews see: a) S. K. Spitzmesser. V. C. Gibson, *Chem. Rev.* **2003**, *103*, 283–315; b) G. J. P. Britovsek, V. C. Gibson, D. F. Wass, *Angew. Chem. Int. Ed.* **1999**, *38*, 429–447.

[2] a) J. D. Scollard, D. H. McConville, *J. Am. Chem. Soc.* **1996**, *118*, 10008–10009; b) J. D. Scollard, D. H. McConville, N. C. Payne, J. J. Vittal, *Macromolecules* **1996**, *29*, 5241–5243.

[3] a) R. Baumann, W. M. Davis, R. R. Schrock, *J. Am. Chem. Soc.* **1997**, *119*, 3830–3831; b) R. R. Schrock, F. Schattenmann, M. Aizenberg, W. M. Davis, *Chem. Commun.* **1998**, 1999–2000; c) R. Baumann, R. R. Schrock, *J. Organomet. Chem.* **1998**, *557*, 69–75; d) R. R. Schrock, R. Baumann, S. M. Reid, J. T. Goodman, R. Stumpf, D. M. Davis, *Organometallics* **1999**, *18*, 3649–3670; e) J. T. Goodman, R. R. Schrock, *Organometallics* **2001**, *20*, 5205–5211.

[4] a) A. Shafir, M. P. Power, G. D. Whitener, J. Arnold, *Organometallics* **2001**, *20*, 1365–1369; b) R. M. Gauvin, C. Lorber, R. Choukroun, B. Donnadieu, J. Kress, *Eur. J. Inorg. Chem.* **2001**, 2337–2346; c) Y. M. Jeon, S. J. Park, J. Heo, K. Kim, *Organometallics* **1998**, *17*, 3161–3163; d) S. Tinkler, R. J. Deeth, D. J. Duncalf, A. McCamley, *J. Chem. Soc. Chem. Commun.* **1996**, 2633–2634; e) , F. G. N. Clocke, T. J. Geldbach, P. B. Hitchcock, J. B. Love, *J. Organomet. Chem.* **1996**, *506*, 343–345; f) N. A. H. Male, M. Thornton-Pett, M. Bochmann, *J. Chem. Soc. Dalton Trans.* **1997**, 2487–2494; g) V. C. Gibson, B. S. Kimberley, A. J. P. White, D. J. Williams, P. Howard, *J. Chem. Soc. Chem. Commun.* **1998**, 313–314; h) C. H. Lee, Y.-H. La, S. J. Park, J. W. Park, *Organometallics* **1998**, *17*, 3648–3655.

[5] a) E. Y. Tshuva, I. Goldberg, M. Kol, *J. Am. Chem. Soc.* **2000**, *122*, 10706–10707; b) E. Y. Tshuva, I. Goldberg, M. Kol, H. Weitman, Z. Goldschmidt, *Chem. Commun.* **2000**, 379–380; c) E. Y. Tshuva, I. Goldberg, M. Kol, Z. Goldschmidt, *Chem. Commun.* **2001**, 2120–2121; d) E. Y. Tshuva, S. Groysman, I. Goldberg, M. Kol, Z. Goldschmidt, *Organometallics* **2002**, *21*, 662–670; e) E. Y. Tshuva, I. Goldberg, M. Kol, Z. Goldschmidt, *Organometallics* **2001**, *20*, 3017–3028; f) E. Y. Tshuva, Goldberg I., M. Kol, Z. Goldschmidt, *Inorg. Chem.* **2001**, *40*, 4263–4270.

[6] a) Y. Nakayama, K. Watanabe, N. Ueyama, A. Nakamura, A. Harada, J. Okuda, *Organometallics* **2000**, *19*, 2498–2503; b) R. M. Gauvin, J. A. Osborn, J. Kress, *Organometallics* **2000**, *19*, 2944–2946; c) H. Mack, M. S. Eisen, *J. Chem. Soc. Dalton Trans.* **1998**, 917–921; d) M. G. Thorn, Z. C. Etheridge, P. E. Fanwick, I. P. Rothwell, *Organometallics* **1998**, *17*, 3636–3638; e) X. Bei, D. C. Swenson, R. F. Jordan, *Organometallics* **1997**, *16*, 3282–3302.

[7] See for example: a) M. Mitani, R. Furuyama, J-I. Mohri, J. Saito, S. Ishii, H. Terao, H. Tanaka, T. Fujita, *J. Am. Chem. Soc.* **2003**, *125*, 4293–4305; b) S. Matsui, Y. Tohi, M. Mitani, J. Saito, H. Makio, H. Tanaka, M. Nitabaru, T. Nakano, T. Fujita, *Chem. Lett.* **1999**, 1065–1066; c) S. Matsui, T. Fujita, *Catal. Today* **2001**, *66*, 63–73; d) J. Saito, M. Mitani, S. Matsui, J-I. Mohri, S. Kojoh, N. Kashiwa, T. Fujita, *Angew. Chem. Int. Ed.* **2001**, *40*, 2918–2920; e) Y. Susuki, N. Kashiwa, T. Fujita, *Chem. Lett.* **2002**, 358–359; f) M. Mitami, T. Nakano, T. Fujita, *Chem. Eur. J.* **2003**, *9*, 2396–2402.

[8] a) J. Tian, G. W. Coates, *Angew. Chem. Int. Ed.* **2000**, *39*, 3626–3629; b) M. Fujita, G. W. Coates, *Macromolecules* **2002**, *35*, 9640–9647; c) J. Tian, P. D. Hustad, G. W. Coates, *J. Am. Chem. Soc.* **2002**, *124*, 3614–3621.

[9] C.-X. Cai, L. Toupet, C. W. Lehmann, J.-F. Carpentier, *J. Organomet. Chem.* **2003**, *683*, 44–55.

[10] a) K. Ziegler, E. Holzkamp, H. Breil, H. Martin, *Angew. Chem.* **1955**, *67*, 426; b) G. Natta, P. Pino, P. Corradini, F. Danusso, E. Mantica, G. Mazzanti, G. Moraglio, *J. Am. Chem. Soc.* **1955**, *77*, 1708–1710.

[11] For recent reviews see: a) G. W. Coates, P. D. Hustad, S. Reinartz, *Angew. Chem. Int. Ed.* **2002**, *41*, 2236–2257; b) H. Hagen, J. Boersma, G. van Koten, *Chem. Soc. Rev.* **2002**, *31*, 357–364; c) S. Gambarotta, *Coord. Chem. Rev.* **2003**, *237*, 229–243.

[12] a) C. Lorber, R. Choukroun, B. Donnadieu, *Inorg. Chem.* **2003**, *42*, 673–675; b) C. Lorber, R. Choukroun, B. Donnadieu, *Inorg. Chem.* **2002**, *41*, 4217–4226; c) R. Choukroun, B. Donnadieu, C. Lorber, P.-M. Pellny, W. Baumann, U. Rosenthal, *Chem. Eur. J.* **2000**, *6*, 4505–4509; d) R. Choukroun, B. Donnadieu, C. Lorber, *Chem. Eur. J.* **2002**, *8*, 2700–2704; e) R. Choukroun, C. Lorber, B. Donnadieu, *Organometallics* **2002**, *21* 1124–1126; f) F. Wolff, R. Choukroun, C. Lorber, B. Donnadieu, *Eur. J. Inorg. Chem.* **2003**, 628–632; g) R. Choukroun, C. Lorber, L. Vendier, B. Donnadieu, *Organometallics* **2004**, *23*, 5488–5492; h) R. Choukroun, C. Lorber, L. Vendier, B. Donnadieu, *Organometallics* **2004**, *23*, 1434–1437; i) C. Lorber, R. Choukroun, L. Vendier, *Organometallics* **2004**, *23*, 1845–1850.

[13] C. Lorber, B. Donnadieu, R. Choukroun, *Organometallics* **2000**, *19*, 1963–1966.

[14] C. Lorber, B. Donnadieu, R. Choukroun, *J. Chem. Soc., Dalton Trans.* **2000**, 4497–4498.

[15] F. Wolff, C. Lorber, R. Choukroun, B. Donnadieu, *Inorg. Chem.* **2003**, *42*, 7839–7845.

[16] F. Wolff, C. Lorber, R. Choukroun, B. Donnadieu, *Eur. J. Inorg. Chem.* **2004**, 2861–2867.

[17] During the course of our study, the crystal structure of $[\text{ONNO}]\text{H}_2$ was reported, but its structural parameters have not been discussed: M. Velusamy, M. Palaniandavar, R. S. Gopalan, G. U. Kulkarni, *Inorg. Chem.* **2003**, *42*, 8283–8293.

[18] N. Desmangles, S. Gambarotta, C. Bensimon, S. Davis, H. Zahalka, *J. Organomet. Chem.* **1998**, *562*, 53–60.

[19] A. K. Atanov, V. C. Gibson, D. Zaher, M. R. J. Elsegood, S. H. Dale, *Chem. Commun.* **2004**, 1956–1957.

[20] a) Y. Doi, S. Ueki, T. Keii, *Macromolecules* **1979**, *12*, 814–819; b) Y. Doi, T. Keii, *Adv. Polymer Sci.* **1986**, *73/74*, 201–209; c) Y. Doi, N. Nomura, K. Ohgizawa, K. Soga, *Makromol. Chem. Rapid Commun.* **1991**, *12*, 245–246.

[21] K. Nomura, A. Sagara, Y. Imanishi, *Macromolecules* **2002**, *35*, 1583–1590.

[22] Pseudo-quantitative ^{13}C NMR spectroscopy allowed us to determined the 1-hexene incorporation ratio into the copolymers by integration of 1-hexene versus ethylene signals, according to Equation (1).

$$\%\ \text{1-hexene} = \frac{1}{1+\frac{1}{2}[(\mathrm{CH_2})_n+\frac{1}{2}\mathrm{C}_\alpha+\mathrm{C}_\beta]} \qquad (1)$$

[23] M. R. Ribeiro, A. Deffieux, M. Fontanille, M. F. Portela, *Macromol. Chem. Phys.* **1995**, *196*, 3833–3844.

[24] a) K. Jokela, A. Väänänen, M. Torkkeli, P. Starck, R. Serimaa, J. Seppälä, *J. Polymer Sci.: Part B: Polym. Phys.* **2001**, *39*, 1860–1875; b) E. Adison, M. Ribeiro, A. Deffieux, M. Fontanille, *Polymer* **1992**, *33*, 4337–4342; c) P. Starck, *Polymer International* **1996**, *40*, 111–122; d) P. Starck, P. Lehmus, J. V. Seppälä, *Polymer Eng. Sci.* **1999**, *39*, 1444–1455; e) M. L. Arnal, V. Balsamo, G. Ronca, A. Sanchez, A. J. Müller, E. Canizales, C. Urbina de Navarro, *J. Thermal Anal. Cal.* **2000**, *59*, 451–470; f) A. Alizadeh, L. Richardson, J. Xu, S. McCartney, H. Marand, Y. W. Cheung, S. Chum, *Macromolecules* **1999**, *32*, 6221–6235; g) K. Czaja, B. Sacher, M. Bialek, *J. Thermal Anal. Cal.* **2002**, *67*, 547–555; h) F. M. Mirabella, *J. polym. Sci. Part B: Polym. Phys.* **2001**, *39*, 2800–2818; i) P. Starck, B. Löfgren, *Eur. Polym. J.* **2002**, *38*, 97–107.

[25] The norbornene content in the copolymers is calculated in a straightforward manner from the four peak groups in the ^{13}C NMR spectrum and by application of the formula in Equation (2), according to: M. Arndt-Rosenau, I. Beulich, *Macromolecules* **1999**, *32*, 7335–7343.

$$\%Norbornene = \frac{\frac{1}{5}[I(C2,C3)+I(C1,C4)+I(C7)]}{\frac{1}{2}[I(C5,C6)+I(C\alpha,C\beta,C\gamma,C\delta)]} = \frac{2}{5}\frac{5N}{2N+2E} = \frac{I(A)+I(B)+I(C)}{2{,}5I(D)} \qquad (2)$$

[26] It is known that the activity of homogeneous vanadium catalysts generally used in the preparation of EPDM (ethylene/propylene/diene terpolymer) can be noticeably increased by means of certain organic halogenated compounds, often called “activators” or “promoters” (such as CCl_4, $CHCl_3$, CH_3CCl_3), that act as oxidizing agent allowing the reoxidation of vanadium(II)-deactivated species into potentially reactivated vanadium(III) ones [see for examples: a) K. Bujadoux. E. Adisson, A. Deffieux, M. Fontanille, *J. Polym. Sci.* **1994**, *32*, 1033–1042; b) S. C. Kao, F. J. Karol (Union Carbide), U. S. Patent 5030605, **1991** [*Chem. Abstr. 115*: 160022e]; c) Ref.[30]

[27] L. E. Manzer, *Inorganic Syntheses* **1982**, *21*, 135–140.

[28] J. J. H. Edema, W. Stauthamer, F. van Bolhuis, S. Gambarotta, W. J. J. Smeets, A. L. Spek, *Inorg. Chem.* **1990**, *29*, 1302–1306.

[29] E. Addison, M. R. Ribeiro, A. Deffieux, M. Fontanille, *Polymer* **1992**, *33*, 4337–4342.

[30] a) A. Altomare, G. Cascarano, C. Giacovazzo, A. Guagliardi, *J. Appl. Cryst.* **1993**, *26*, 343–350; b) A. Altomare, M. C. Burla, M. Camalli, G. L. Cascarano, G. Giacovazzo, A. Guagliardi, A. G. G. Moliterni, G. Polidori, R. Spagna, *J. Appl. Crystallogr.* **1999**, *32*, 115–119.

[31] G. M. Sheldrick, *SHELX97 [includes SHELXS97, SHELXL97, CIFTAB], Programs for Crystal Structure Analysis (Release 97–2)*, Institüt für Anorganische Chemie, Universität Göttingen, **1998**.

[32] L. J. Farrugia, *J. Appl. Crystallogr.* **1999**, *32*, 837–838.

[33] N. Walker, D. Stuart, *Acta Crystallogr. A* **1983**, *39*, 158–166.

Received: February 18, 2005